

Nonadditive intermolecular forces in Ar_n–HF van der Waals clusters: Effects on the HF vibrational frequency shift

Jeremy M. Hutson, Suyan Liu, Jules W. Moskowitz, and Zlatko Bačić

Citation: *The Journal of Chemical Physics* **111**, 8378 (1999); doi: 10.1063/1.480179

View online: <http://dx.doi.org/10.1063/1.480179>

View Table of Contents: <http://scitation.aip.org/content/aip/journal/jcp/111/18?ver=pdfcov>

Published by the [AIP Publishing](#)

Articles you may be interested in

[Ar_n HF van der Waals clusters revisited: II. Energetics and HF vibrational frequency shifts from diffusion Monte Carlo calculations on additive and nonadditive potential-energy surfaces for n = 1 - 12](#)

J. Chem. Phys. **123**, 054305 (2005); 10.1063/1.1991856

[Ar_n HF van der Waals clusters revisited. I. New low-energy isomeric structures for n=6–13](#)

J. Chem. Phys. **121**, 11045 (2004); 10.1063/1.1811612

[Hybrid diatomics-in-molecules-based quantum mechanical/molecular mechanical approach applied to the modeling of structures and spectra of mixed molecular clusters Ar_n \(HCl\)_m and Ar_n \(HF\)_m](#)

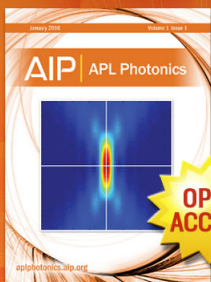
J. Chem. Phys. **120**, 3732 (2004); 10.1063/1.1642596

[Clusters containing open-shell molecules. II. Equilibrium structures of Ar_n OH Van der Waals clusters \(X 2 Π, n=1 to 15\)](#)

J. Chem. Phys. **117**, 4777 (2002); 10.1063/1.1497966

[Non-additive intermolecular forces from the spectroscopy of Van der Waals trimers: A comparison of Ar₂–HF and Ar₂–HCl, including H/D isotope effects](#)

J. Chem. Phys. **106**, 6288 (1997); 10.1063/1.473645



Launching in 2016!

The future of applied photonics research is here

OPEN
ACCESS

AIP | APL
Photonics

Nonadditive intermolecular forces in $\text{Ar}_n\text{-HF}$ van der Waals clusters: Effects on the HF vibrational frequency shift

Jeremy M. Hutson^{a)}

Department of Chemistry, University of Durham, South Road, Durham, DH1 3LE, United Kingdom

Suyan Liu, Jules W. Moskowitz, and Zlatko Bačić^{b)}

Department of Chemistry, New York University, New York, New York 10003

(Received 16 July 1999; accepted 13 August 1999)

The effects of nonadditive forces on $\text{Ar}_n\text{-HF}$ van der Waals clusters are investigated for $n=2, 3, 4,$ and 12 . The pair potentials operating in these systems are accurately known. Earlier models of nonadditive forces in $\text{Ar}_2\text{-HF}$, including nonadditive dispersion, induction, and overlap distortion, are generalized to handle clusters of arbitrary size. Calculations of vibrational frequency shifts (redshifts) are then performed and compared with experiment. The geometries of the clusters are first optimized by simulated annealing; the Ar_n cage is then held fixed, and the resulting five-dimensional Schrödinger equation is solved for the hindered rotational and translational motion of the HF molecule in the field of the Ar atoms. The nonadditive potentials are found to account remarkably well for the observed frequency shifts. © 1999 American Institute of Physics.

[S0021-9606(99)00142-7]

I. INTRODUCTION

The physical behavior of atomic and molecular liquids is largely controlled by intermolecular forces. If the intermolecular forces are completely known, then molecular dynamics or Monte Carlo simulations may in principle be used to predict physical properties. However, there are in fact very few systems for which the potential energy surfaces are accurate enough for such calculations to have predictive power. Even if the intermolecular pair potentials are known accurately, there are substantial contributions from nonadditive forces, and not much is known about these except for purely atomic systems. It is common to carry out simulations using effective pair potentials that are supposed to incorporate the nonadditive effects in some averaged way, but such an approach loses the connection with detailed studies of intermolecular potentials based on molecular scattering, van der Waals complexes, or *ab initio* calculations.

In recent years, atomic and molecular clusters have started to provide a more systematic framework for studying additive and nonadditive intermolecular forces. High-resolution spectra of van der Waals complexes have been used to determine accurate and reliable anisotropic pair potentials for systems such as Ar-HF ¹ and Ar-HCl .² These potentials have been shown to perform well for newly measured properties such as the parameters of additional bands in the spectra of the van der Waals complexes,^{3,4} inelastic cross sections,⁵ and infrared pressure broadening coefficients.⁶ The potentials have also been used to calculate the spectra of van der Waals trimers such as $\text{Ar}_2\text{-HF}$ and $\text{Ar}_2\text{-HCl}$.⁷⁻¹¹ When pairwise additivity was assumed, the accurate pair potentials were found to give predicted bending

frequencies for HX hindered rotational bands of the trimers that were substantially below the measured frequencies. The discrepancies were considerably larger than could be attributed to uncertainties in the pair potentials, and have been interpreted in terms of nonadditive forces. However, conventional types of nonadditive force (dispersion, exchange overlap, etc.) were found to be inadequate to explain the discrepancies. It was found necessary to include a new type of nonadditive force,⁷ which arises because the two Ar atoms distort away from one another when they approach close together, creating a quadrupole moment on the Ar_2 pair. This “exchange quadrupole” moment has a strong electrostatic interaction with the permanent multipole moments of the HX molecule.

In addition to the HX bending frequencies of the trimers, McIlroy *et al.*¹² have measured redshifts for the HF fundamental mode in $\text{Ar}_n\text{-HF}$ clusters for $n=1$ to 4 . The redshift for $n=1$ (9.654 cm^{-1}) was among the data used to determine the Ar-HF pair potential, so it is well reproduced. The measured redshift for $n=2$ is 14.827 cm^{-1} , while that calculated for the pairwise-additive potential is 15.355 cm^{-1} .¹¹ Note that this is *not* simply twice the value for $n=1$: pairwise additivity for the potential does not produce pairwise additivity in the redshift. The discrepancy of 0.53 cm^{-1} is probably due mostly to nonadditive forces.

The most recent version of the models for the nonadditive forces is that of Ernesti and Hutson,¹¹ who developed two slightly different models for the nonadditive forces, including nonadditive dispersion, induction, and the electrostatic forces due to exchange overlap. These models perform reasonably well for HX bending frequencies and for vibrational redshifts in both $\text{Ar}_2\text{-HF}$ and $\text{Ar}_2\text{-HCl}$; for $\text{Ar}_2\text{-HF}$, they give redshifts of 14.580 and 14.476 cm^{-1} . This agreement with experiment is reasonably satisfactory: the remaining discrepancies of around 0.25 or 0.35 cm^{-1} probably in-

^{a)}Electronic mail: J.M.Hutson@durham.ac.uk

^{b)}Electronic mail: Zlatko.Bacic@nyu.edu

dicates that the models overcorrect for nonadditivity, though part of the discrepancies may be due to deficiencies in the pair potentials.

It is of great interest to explore how the nonadditive contributions to redshifts extrapolate to larger clusters. However, the quantum-mechanical bound-state methods used by Ernesti and Hutson are not readily extended beyond van der Waals trimers. Bačić and co-workers have described two approaches capable of handling larger clusters.¹³ In the first approach, the equilibrium structure of the cluster is found by simulated annealing;¹⁴ the positions of the Ar atoms are then held fixed, and the five-dimensional (5D) Schrödinger equation for hindered rotation and translation of the HX molecule in the field of the Ar atoms is solved.^{15,16} The simulated annealing approach has been applied for Ar_n-HF clusters up to $n=14$, using pairwise-additive potentials;¹⁴ it was found that the HX molecule sits on the outside of an Ar_n cluster up to $n=8$, but then moves inside. In particular, the Ar₁₂-HF cluster has an HF molecule surrounded by a near-spherical (icosahedral) shell of 12 Ar atoms. Within this methodology, vibrational redshifts can be calculated by performing separate 5D calculations on potential energy surfaces corresponding to the $v=0$ and 1 states of HX.^{15,16}

The simulated annealing/5D quantum approach can be applied to fairly large clusters, and can in principle provide energy levels for both the ground state and for excited hindered rotational states of HX in the cluster. However, it is inherently approximate because all Ar-Ar motions are neglected. Niyaz *et al.*¹⁷ have therefore used an alternative approach, using diffusion quantum Monte Carlo (DQMC) calculations including all vibrational degrees of freedom in a fully coupled manner. This provides energy levels only for van der Waals ground states, but is in principle exact (except for statistical sampling errors). It is also substantially more expensive than the five-dimensional fixed-Ar calculation, and has so far been applied to clusters with n up to 4 (again for pairwise-additive potentials).

The redshifts obtained from calculations on pairwise-additive potentials are consistently larger than the experimental values: the differences obtained from 5D^{15,16} (or DQMC¹⁷) calculations are 0.8 (or 0.6), 1.8 (or 1.3), and 2.0 (or 1.4) cm⁻¹ for $n=2, 3$, and 4, respectively. In view of the high quality of the pair potentials used, these differences can be attributed principally to the nonadditive interactions and provide useful tests of models of the nonadditivity.

The purpose of the present work is to extend the cluster calculations to include nonadditive forces, in order to allow comparisons with experiment and understand how the nonadditive forces build up with cluster size.

II. MODELS FOR THE POTENTIAL ENERGY SURFACE

All the potential surfaces used in the present work are made up of pairwise-additive and nonadditive components.

A. Pairwise-additive potentials

The pair potentials used in the present work are:

- (a) The Ar-Ar HFD-C potential of Aziz and Chen,¹⁸

which is used here for consistency with the earlier work of Liu *et al.*¹⁶ Ernesti and Hutson¹¹ used the quite similar HFDID1 potential of Aziz.¹⁹ These potentials are the most recent fits to a wide range of experimental data, including both bulk properties (such as second virial coefficients and transport coefficients) and microscopic properties (such as molecular beam scattering results and vibration-rotation energy levels). They both give highly accurate vibrational frequencies and rotational constants for the Ar dimer.

- (b) The Ar-HF H6(4,3,2) potential of Hutson.¹ This potential energy surface was fitted to spectroscopic constants obtained from 24 different bands in the microwave, far-infrared, and mid-infrared spectra of Ar-HF ($v=0, 1$ and 2) and Ar-DF ($v=0$ and 1). The potential includes both the anisotropy and the dependence on the vibrational state v of the HF molecule; the latter is built in parametrically, in terms of the mass-reduced vibrational quantum number,

$$\eta = (v + \frac{1}{2}) / \mu_{\text{HF}}^{1/2}, \quad (1)$$

where μ_{HF} is the reduced mass of the HF molecule.

These potentials are used to construct v -dependent pairwise-additive potential energy surfaces for Ar_n-HF clusters.

B. Nonadditive forces

Ernesti and Hutson¹¹ have previously described two models for the nonadditive intermolecular forces in clusters such as Ar₂-HF and Ar₂-HCl. Their models include nonadditive dispersion, induction, and the electrostatic forces due to exchange overlap effects. The exchange overlap effect is modeled in terms of dipole moments on the two Ar atoms, and interference between dipoles arising from this source and those resulting from induction is allowed. In a larger cluster, more extensive interference can occur, so that it would not be appropriate simply to use the three-body model and sum it over all triples in a larger cluster. Instead, it is better to construct an n -body model that embodies the same physical principles. This is the objective of the present section.

1. Dispersion contributions

In atomic systems, the most important nonadditive forces are those arising from dispersion. The leading term in the three-body dispersion interaction is the well-known Axilrod-Teller triple-dipole term,²⁰ which for atomic systems takes the form

$$V_{\text{ddd}} = 3Z_{\text{ddd}}^{(3)} \left(\frac{3 \cos \theta_1 \cos \theta_2 \cos \theta_3 + 1}{r_1^3 r_2^3 r_3^3} \right), \quad (2)$$

where r_1 , r_2 , and r_3 are the lengths of the sides of the triangle formed by the three atoms and θ_1 , θ_2 , and θ_3 are the corresponding internal angles of the triangle. The coefficients $\nu_{123} = 3Z_{\text{ddd}}^{(3)}$ were taken to be $269.9 E_h a_0^9$ for Ar₂-HF²¹ and $530 E_h a_0^9$ for Ar₃. However, this Ar₂-HF value is appropriate for $r=r_e$ (corresponding to a mass-reduced quantum number $\eta=0$), and we require a coefficient that includes the dependence on η . In the present work, we

have assumed that the Axilrod-Teller coefficient has the same η -dependence as the Ar–HF C_6 coefficient of Ref. 1, so that

$$\nu_{123}(\eta) = \nu_{123}(0)[1 + 0.0239\eta/m_u^{-1/2}], \quad (3)$$

where m_u is the unified atomic mass unit.

In molecular systems, the triple-dipole interaction is much more complicated because of the anisotropy of molecular polarizabilities. An approximate form for the triple-dipole energy under these circumstances has been given by Stogryn,²²

$$V_{DDD} = \frac{\nu_{123}}{3\bar{\alpha}_1\bar{\alpha}_2\bar{\alpha}_3} (T_{12})_{\alpha\beta} (T_{23})_{\gamma\delta} (T_{31})_{\mu\nu} \\ \times (\alpha_1)_{\nu\alpha} (\alpha_2)_{\beta\gamma} (\alpha_3)_{\delta\mu}, \quad (4)$$

where α_i is the polarizability tensor and $\bar{\alpha}_i$ is the mean polarizability for particle i . T_{ij} is a symmetric orientation tensor, with Cartesian components

$$(T_{ij})_{\alpha\beta} = \frac{3(\hat{r}_{ij})_{\alpha}(\hat{r}_{ij})_{\beta} - \delta_{\alpha\beta}}{|r_{ij}|^3}, \quad (5)$$

and $(\hat{r}_{ij})_{\alpha}$ is the component of the unit vector between particles i and j along Cartesian axis α . Equation (4) uses the usual summation convention, summing over all repeated suffices representing Cartesian axes. In the present work, it was found to be most convenient to evaluate Eq. (4) in a Cartesian axis system with the z axis along the HF bond, since in this axis system the polarizability tensors are diagonal and only three nested DO loops are needed to evaluate the sum for each Ar–Ar–HF triple.

In the present work, V_{DDD} was evaluated in two different ways. In the first, all the HF dispersion was treated as arising from a single center of polarizability placed at the HF center of mass. The quantity $V_{DDD}^{(1)}$ was evaluated by summing Eqs. (2) and (4) over all Ar₃ and Ar₂–HF triples in the Ar_{*n*}–HF cluster, using $\alpha_{\text{Ar}} = 11.096 a_0^3$ (Ref. 23) and the η -dependent HF polarizabilities $\alpha_{\parallel}(\eta)$ and $\alpha_{\perp}(\eta)$ of Ref. 1.

The single-center model is the three-body analog of a two-body dispersion model that places all the dispersion at the HX center of mass and completely neglects odd-order (non-centrosymmetric) terms in the dispersion expansion. In the two-body case, this may be improved by moving a part of the HX polarizability (and hence dispersion) from the center of mass to a point halfway along the HX bond. As described by Douketis *et al.*,²⁴ this may be done in a way that gives the correct angle-dependent C_7R^{-7} terms in the pair potential. For HF, the total ν -dependent polarizability and its anisotropy are split into parts at the HF center of mass ($\bar{\alpha}_X$ and $\Delta\alpha_X$) and parts at the HF bond midpoint ($\bar{\alpha}_M$ and $\Delta\alpha_M$). As an illustration, for $\nu=0$ the total HF polarizability ($\bar{\alpha}=5.601 a_0^3$ and $\Delta\alpha=1.440 a_0^3$) is split into components $\bar{\alpha}_X=4.028 a_0^3$ and $\Delta\alpha_X=-0.859 a_0^3$ at the center of mass and $\bar{\alpha}_M=1.573 a_0^3$ and $\Delta\alpha_M=2.299 a_0^3$ at the bond midpoint. The quantity $V_{DDD}^{(2)}$, representing the two-site model of the

nonadditive triple-dipole energy, is evaluated as for the single-site model, but with Eq. (4) evaluated separately for the X and M sites.¹¹

For pair potentials, it is well known that the dispersion interaction must be damped when overlap is significant, to prevent the inverse power terms dominating the potential at short range. In principle, analogous damping functions are needed for nonadditive dispersion terms.^{25,26} However, damping functions for three-body interactions are not as well understood as for pair potentials, and it was found for Ar₂–HCl⁷ that damping the triple-dipole term in a plausible way had little effect on the bending energy levels. Accordingly, the triple-dipole formula was used without damping in the present work.

2. Induction contributions

In a polar liquid such as water, the nonadditivity is dominated by the induction energy: the polarization energy of each molecule depends on the square of the electric field due to all the other molecules, and the different electric fields must be added vectorially before the resultant is squared. However, this mechanism does not operate in a cluster such as Ar_{*n*}–HF that contains only one polar molecule.

There is nevertheless a nonadditive induction energy in Ar_{*n*}–HF. The highly polar HF molecule creates a substantial electric field at the location of each Ar atom. These fields (and the corresponding field gradients) polarize the Ar atoms, producing induced dipole moments (and higher multipoles). The direct interactions between the induced moments and the permanent moments of the HF are already taken into account in the Ar–HF pair potential, but there is a nonadditive energy contribution arising from the interactions between the induced moments on the different Ar atoms. In the present work, the electric field at each Ar atom is evaluated including HX multipole moments up to hexadecapole. The values used for the multipole moments are given below.

If induction were the *only* effect to produce dipole moments on the Ar atoms, the interaction energy of each pair of induced dipoles could be calculated from

$$V_{\text{ind}} = -[3(\boldsymbol{\mu}_1^{\text{ind}} \cdot \hat{\boldsymbol{\rho}})(\boldsymbol{\mu}_2^{\text{ind}} \cdot \hat{\boldsymbol{\rho}}) - \boldsymbol{\mu}_1^{\text{ind}} \cdot \boldsymbol{\mu}_2^{\text{ind}}]/\rho^3, \quad (6)$$

where $\hat{\boldsymbol{\rho}}$ is a unit vector along the Ar–Ar axis. However, as discussed previously,¹⁰ there are additional Ar dipoles arising from short-range effects, so that a slightly more sophisticated treatment is needed as discussed below.

3. Overlap-dependent contributions

In previous work, we considered short-range nonadditive forces arising from two different sources.

First, there is a short-range term analogous to that for Ar₃, termed the exchange overlap contribution:²⁷ when two atoms or molecules approach one another closely, their electron clouds distort away from one another in such a way as to reduce overlap. This distortion modifies their overlap with a third body; if the third body is near the axis of the first two, the overlap is increased and there is a positive contribution to the three-body energy. Conversely, for near-equilateral geometries, the deformation produces a negative contribution

to the three-body energy. Earlier work on Ar₂-HCl⁷ showed that the exchange overlap term makes very small contributions to the nonadditive shifts; accordingly, it has not been included in the present study.

Second, as described above, two Ar atoms *i* and *j* that are close together distort, producing a quadrupole moment on the Ar₂ pair. This quadrupole can interact with the permanent multipoles of the HF molecule. In addition, the dispersion interaction between the two Ar atoms creates a pair quadrupole of the opposite sign. We have shown previously¹⁰ that the quadrupole moment $\Theta(\rho)$ (dependent on the Ar-Ar distance ρ_{ij}) is best represented in terms of contributions μ_i^{eqd} to the dipoles on the Ar atoms,

$$\mu_i^{\text{eqd}} = \sum_{j \neq i} \mu_{ij}^{\text{eqd}}, \quad (7)$$

where the superscript eqd indicates exchange quadrupole + dispersion and

$$\mu_{ij}^{\text{eqd}} = -\mu_{ji}^{\text{eqd}} = \frac{1}{2} \Theta(\rho_{ij}) \hat{\rho}_{ij} / \rho_{ij}. \quad (8)$$

The quadrupole moment $\Theta(\rho)$ of the Ar₂ pair is evaluated using the functional form

$$\Theta(\rho) = -\frac{1}{2} e \rho^2 \frac{\exp(-\frac{1}{2} \beta_{\text{eq}}^2 \rho^2)}{1 - \exp(-\frac{1}{2} \beta_{\text{eq}}^2 \rho^2)} + \Theta_6 / \rho^6. \quad (9)$$

The first term in Eq. (9) is termed the exchange quadrupole (eq) contribution, and is represented here using a functional form derived by Jansen²⁸ from a single-electron approximation. However, Jansen's value of β_{eq} is known to produce a substantial overestimate of the exchange quadrupole, so we used instead a value $\beta_{\text{eq}} = 0.936 \text{ \AA}^{-1}$, obtained by fitting to self-consistent field (SCF) calculations of the short-range overlap quadrupole of Ar₂.²⁹ The second term in Eq. (9) arises from dispersion:³⁰ in the present work the quadrupole dispersion coefficient is taken to be $\Theta_6 = 2086 ea_0^8$, as explained in Ref. 10. The dispersion contribution to $\Theta(\rho)$ is of opposite sign to the exchange quadrupole term, and about 30% as large at the equilibrium geometry.

The Ar-Ar exchange effect and the induction both produce dipole moments on the Ar atoms. In the present work, we calculate the vector sum of the dipole contributions on each atom,

$$\mu_i^{\text{tot}} = \mu_i^{\text{ind}} + \sum_{j \neq i} \mu_{ij}^{\text{eqd}}, \quad (10)$$

where the sum over *j* runs over all other Ar atoms in the cluster. The energies of interaction between every pair of Ar dipoles and between each of them and the multipole moments on the HX molecule are easily calculated. However, care is needed to avoid double counting: all contributions that are part of the Ar-Ar and Ar-HX pair potentials must be excluded from the nonadditive terms. The interactions between μ_i^{ind} and the HX multipoles and between μ_{ij}^{eqd} and μ_{ji}^{eqd} are of this type. The resulting *n*-body contribution is thus

$$\begin{aligned} V_3 = & - \sum_i \mathbf{F}_i \cdot \mu_i^{\text{eqd}} \\ & - \sum_{i>j} [3(\mu_i^{\text{tot}} \cdot \hat{\rho}_{ij})(\mu_j^{\text{tot}} \cdot \hat{\rho}_{ij}) - \mu_i^{\text{tot}} \cdot \mu_j^{\text{tot}}] / \rho_{ij}^3 \\ & + \sum_{i>j} [3(\mu_{ij}^{\text{eqd}} \cdot \hat{\rho}_{ij})(\mu_{ji}^{\text{eqd}} \cdot \hat{\rho}_{ij}) - \mu_{ij}^{\text{eqd}} \cdot \mu_{ji}^{\text{eqd}}] / \rho_{ij}^3. \end{aligned} \quad (11)$$

Since in Ar₂ μ_{ij}^{eqd} and μ_{ji}^{eqd} are directed along $\hat{\rho}_{ij}$ and are equal and opposite, the last term simplifies to $-2 \sum_{i>j} |\mu_{ij}^{\text{eqd}}|^2 / \rho_{ij}^3 = -\sum_{i>j} 1/2 [\Theta(\rho_{ij})]^2 / \rho_{ij}^5$.

The first term in Eq. (11) is calculated with the HF charge distribution represented by a single-center multipole expansion, including multipoles up to the hexadecapole at the HF center of mass, as described for the induction term above.

The dependence of the nonadditive terms on the HF vibrational level *v* is easily built in by using *v*-dependent (or η -dependent) values of the HF multipole moments Q_l . In the present work, the HF dipole and quadrupole were represented using the η -dependent functions given in Table I of Ref. 1, and the HF octopole and hexadecapole were taken from the configuration interaction calculations of Amos,³¹ $\Phi_{\text{HF}} = 2.4466 ea_0^3$ and $\Omega_{\text{HF}} = 4.7382 ea_0^4$. The η -dependence of the octopole and hexadecapole was neglected.

4. The total nonadditive potentials

Two different nonadditive potentials are used in the present work, designated "Total 1" and "Total 2." They both use the same model for the induction and overlap-dependent contributions as described above. They differ only in their treatment of the dispersion contribution: the "Total 1" model uses the single-site model of the nonadditive dispersion, while the "Total 2" model uses a two-site model, with dispersion sites on the HF center of mass and at the HF bond midpoint.

III. COMPUTATIONAL METHODS

The results presented in this work were obtained using the quantum 5D methodology developed previously^{13,16} for calculating vibrational frequency shifts of diatomic molecules microsolvated by rare gas atoms. Since a detailed description of this methodology is available,¹⁶ we summarize here only its key steps:

- (i) The equilibrium geometries of the isomers of an Ar_n-HF cluster are determined by finding the minima of the intermolecular potential energy surface (IPES) of the cluster. This is done separately for HF *v*=0 and *v*=1, and the resulting minima are denoted $V_{n,i}^v$. The geometries of the global minima (*i*=1) and secondary local minima (*i*>1) depend very weakly on *v*. The cluster geometry optimization is carried out by simulated annealing followed by a direct minimization scheme.¹⁴

TABLE I. Calculated energies [relative to $(n+1)$ -body dissociation] and vibrational redshifts for the HF fundamental vibration from simulated annealing and 5D quantum calculations on Ar_n -HF clusters. All quantities are in cm^{-1} .

		Minimum energy			5D, Ar fixed			Experiment
		Pairwise	Total 1	Total 2	Pairwise	Total 1	Total 2	
$n=2$	$\nu=0$	-424.08	-406.33	-404.72	-302.28	-294.54	-294.09	
	$\nu=1$	-447.17	-428.32	-426.45	-317.88	-309.33	-308.77	
	Redshift	23.12	21.99	21.73	15.60	14.78	14.68	14.827
$n=3$	$\nu=0$	-736.61	-691.82	-688.40	-605.70	-580.03	-578.79	
	$\nu=1$	-764.75	-717.79	-713.87	-626.81	-599.28	-597.78	
	Redshift	28.14	25.97	25.47	21.11	19.25	18.99	19.260
$n=4$	$\nu=0$	-1046.60	-984.90	-980.93	-913.73	-874.53	-873.12	
	$C_{3\nu}$ $\nu=1$	-1075.31	-1011.21	-1006.67	-935.45	-894.10	-892.39	
	Redshift	28.71	26.31	25.74	21.72	19.57	19.27	19.697
$n=4$	$\nu=0$		-972.37	-969.77	-907.83	-868.00	-866.56	
	$C_{2\nu}$ $\nu=1$		-999.62	-996.68	-932.12	-890.02	-888.15	
	Redshift		27.25	26.91	24.29	22.02	21.59	
$n=12$	$\nu=0$	-4430.06	-4224.73	-4224.21	-4337.28	-4133.94	-4133.17	
	$\nu=1$	-4474.76	-4266.19	-4265.67	-4379.73	-4173.14	-4172.18	
	Redshift	44.70	41.46	41.46	42.46	39.20	39.01	

- (ii) The Ar_n subunit is *frozen* in the geometry of the i th Ar_n -HF minimum $V_{n,i}^{\nu}$ (slightly different for HF $\nu=0$ and $\nu=1$). With this restriction, the Ar_n -HF cluster becomes a weakly bound *dimer* whose two monomers are the rigid Ar_n microcluster and the HF molecule. The 5D IPES of this dimer, which governs its intramolecular vibrations, depends on the geometry of the Ar_n subunit and is therefore different for each Ar_n -HF isomer.
- (iii) The 5D intermolecular vibrational levels of the floppy Ar_n -HF dimer are calculated separately for HF $\nu=0$ and $\nu=1$, by an efficient quantum 5D bound-state method.¹⁶ The quantum 5D intermolecular vibrational ground-state energies of the dimer, for HF $\nu=0$ and 1 and Ar_n geometries defined by the minima $V_{n,i}^{\nu}$, are designated $E_{n,i}^0$ and $E_{n,i}^1$, respectively.
- (iv) In the 5D approximation, the HF vibrational frequency shift for the i th isomer of Ar_n -HF is obtained as the difference between $E_{n,i}^1$ and $E_{n,i}^0$.

IV. RESULTS AND DISCUSSION

The equilibrium energies (from simulated annealing) and the ground-state energies (from five-dimensional fixed-Ar calculations) are shown in Table I, for Ar_n -HF clusters with HF in $\nu=0$ and 1. The redshifts on pairwise-additive and nonadditive potential surfaces are compared with experimental values for clusters with $n=2, 3$, and 4 Ar atoms.

As shown previously,¹⁵ the 5D redshifts from pairwise-additive potentials are consistently too large, by about 0.8, 1.8, and 2.0 cm^{-1} for $n=2, 3$, and 4, respectively. Table I shows that the ‘‘Total 1’’ (single-center dispersion) model of the nonadditivity corrects these almost exactly: the remaining discrepancies are only -0.05 , -0.01 , and -0.13 cm^{-1} ,

respectively. The ‘‘Total 2’’ (distributed dispersion) model overcorrects by rather more, giving a redshift that is 0.4 cm^{-1} too small for $n=4$.

The agreement with experiment is to some extent fortuitous: Niyaz *et al.*¹⁷ have shown that, for pairwise potentials, replacing the 5D calculations with DQMC calculations including all degrees of freedom reduces the redshifts by between 0.2 and 0.5 cm^{-1} . Test DQMC calculations³² confirm that the changes are much the same for the nonadditive potentials. It thus seems that even the Total 1 model overestimates the nonadditive corrections by about these amounts.

For Ar_4 -HF, there is both a $C_{3\nu}$ isomer (with the fourth argon capping the original Ar_3 triangle to form an Ar_4 tetrahedron) and a $C_{2\nu}$ isomer (with two Ar atoms capping the triangular faces of T-shaped Ar_2 -HF) as shown in Fig. 2 of Ref. 14. On the pairwise potential, the $C_{3\nu}$ ground state (from 5D calculations) lies 5.9 cm^{-1} below the $C_{2\nu}$ ground state. This energy difference is only slightly reduced (to between 5.5 and 5.7 cm^{-1}) on the nonadditive potentials. The difference in redshifts for the two isomers, which is 2.6 cm^{-1} on the pairwise potential, is reduced by only about 0.2 cm^{-1} on the nonadditive potentials.

There have been various other calculations of the nonadditive contributions to cluster redshifts. However, none of them have included the nonadditive induction and exchange overlap effects, which earlier work has shown to be the dominant nonadditive effects in Ar_2 -HF.¹⁰ Lewerenz³³ has carried out DQMC calculations, using the same pair potentials as in the present work but with a much simpler nonadditive potential (based on isotropic Axilrod-Teller interactions, with no vibrational dependence). Lewerenz found that such a nonadditive term actually increased the redshifts, making the agreement with experiment poorer rather than better. Dykstra³⁴ has also carried out DQMC calculations, for

clusters up to Ar₁₂-HF: he used simple model pair potentials, again with Axilrod-Teller nonadditive terms. He considered mutual polarization (our nonadditive induction) at specific geometries, but did not include it in the DQMC calculations. He also took no account of the exchange quadrupoles. Dykstra's model pair potentials gave a redshift of 17.68 cm⁻¹ for Ar₂-HF, which is 2.85 cm⁻¹ greater than the experimental value (and thus in error by a factor of 5 more than ours at the DQMC level). He adjusted his Axilrod-Teller term to match the Ar₂-HF and Ar₃-HF redshifts as well as possible, giving values of 15.22 cm⁻¹ (0.39 cm⁻¹ too large) and 18.63 cm⁻¹ (0.63 cm⁻¹ too small), respectively. We believe that, by using poor pair potentials and neglecting other nonadditive terms, Dykstra obtained far too large a value for the Axilrod-Teller contribution to the redshift; this is manifested in his prediction for the redshift for Ar₁₂-HF, 18.83 cm⁻¹, which may be contrasted with our value of 39.20 cm⁻¹ from 5D calculations on the "Total 1" nonadditive potential.

The redshift for the Ar₁₂-HF cluster has not yet been measured, but the redshift for HF in an Ar matrix has: it is 42.4 cm⁻¹.¹² This is very close to the value obtained from 5D calculations on our pairwise potential,^{15,35} 42.46 cm⁻¹. However, such comparisons must be made with care, and Schmidt and Jungwirth³⁶ have given a careful analysis of the effects involved. For example, HF in an Ar matrix occupies an octahedral rather than an icosahedral site: the calculated redshift is about 4 cm⁻¹ less at an octahedral site than at an icosahedral site (largely because the octahedrally arranged Ar atoms are farther from the HF). However, the redshift increases when additional solvent shells are added, and is about 7 cm⁻¹ larger in the bulk matrix than for a single octahedral shell. Combining these two corrections, the measured matrix shift of 42.4 cm⁻¹ might be taken to imply a value around 39.4 cm⁻¹ for Ar₁₂-HF. This is in remarkably good agreement with the values of 39.2 and 39.4 cm⁻¹ calculated with our two models of the nonadditive forces.

V. CONCLUSIONS

We have investigated the effects of nonadditive intermolecular forces on the vibrational redshifts for Ar_n-HF clusters, and have compared the results with experimental values. We have generalized the models of nonadditivity proposed by Ernesti and Hutson to handle clusters containing more than two Ar atoms. We find that the models give a remarkably good account of the experimental frequency shifts. The simpler of the two models, with a single dispersion site on the HF molecule, performs rather better for these systems than the more sophisticated version with a distributed model of the nonadditive dispersion.

ACKNOWLEDGMENTS

We are grateful to Dr. Parhat Niyaz for carrying out DQMC calculations, using the nonadditive potential energy surfaces, to verify that the 5D calculations described here are reliable. Zlatko Bačić is grateful to the National Science Foundation for partial support of this research through Grant No. CHE-9613641.

- ¹J. M. Hutson, *J. Chem. Phys.* **96**, 6752 (1992).
- ²J. M. Hutson, *J. Phys. Chem.* **96**, 4237 (1992).
- ³C. M. Lovejoy, J. M. Hutson, and D. J. Nesbitt, *J. Chem. Phys.* **97**, 8009 (1992).
- ⁴H.-C. Chang, F.-M. Tao, W. Klemperer, C. Healey, and J. M. Hutson, *J. Chem. Phys.* **99**, 9337 (1993).
- ⁵W. B. Chapman, M. J. Weida, and D. J. Nesbitt, *J. Chem. Phys.* **106**, 2248 (1997).
- ⁶S. Green and J. M. Hutson, *J. Chem. Phys.* **100**, 891 (1994).
- ⁷A. R. Cooper and J. M. Hutson, *J. Chem. Phys.* **98**, 5337 (1993).
- ⁸M. J. Elrod, R. J. Saykally, A. R. Cooper, and J. M. Hutson, *Mol. Phys.* **81**, 579 (1994).
- ⁹A. Ernesti and J. M. Hutson, *Faraday Discuss. Chem. Soc.* **97**, 119 (1994).
- ¹⁰A. Ernesti and J. M. Hutson, *Phys. Rev. A* **51**, 239 (1995).
- ¹¹A. Ernesti and J. M. Hutson, *J. Chem. Phys.* **106**, 6288 (1997).
- ¹²A. McIlroy, R. Lascola, C. M. Lovejoy, and D. J. Nesbitt, *J. Phys. Chem.* **95**, 2636 (1991).
- ¹³Z. Bačić, *J. Chem. Soc., Faraday Trans.* **93**, 1459 (1997).
- ¹⁴S. Liu, Z. Bačić, J. W. Moskowitz, and K. E. Schmidt, *J. Chem. Phys.* **100**, 7166 (1994).
- ¹⁵S. Liu, Z. Bačić, J. W. Moskowitz, and K. E. Schmidt, *J. Chem. Phys.* **101**, 10181 (1994).
- ¹⁶S. Liu, Z. Bačić, J. W. Moskowitz, and K. E. Schmidt, *J. Chem. Phys.* **103**, 1829 (1995).
- ¹⁷P. Niyaz, Z. Bačić, J. W. Moskowitz, and K. E. Schmidt, *Chem. Phys. Lett.* **252**, 23 (1996).
- ¹⁸R. A. Aziz and H. H. Chen, *J. Chem. Phys.* **67**, 5719 (1977).
- ¹⁹R. A. Aziz, *J. Chem. Phys.* **99**, 4518 (1993).
- ²⁰B. M. Axilrod and E. Teller, *J. Chem. Phys.* **11**, 299 (1943).
- ²¹A. Kumar and W. J. Meath, *Mol. Phys.* **54**, 823 (1985).
- ²²D. E. Stogryn, *Phys. Rev. Lett.* **24**, 971 (1970).
- ²³E.-A. Reinsch and W. Meyer, *Phys. Rev. A* **14**, 915 (1976).
- ²⁴C. Douketis, J. M. Hutson, B. J. Orr, and G. Scoles, *Mol. Phys.* **52**, 763 (1984).
- ²⁵S. F. O'Shea and W. J. Meath, *Mol. Phys.* **28**, 1431 (1974).
- ²⁶S. F. O'Shea and W. J. Meath, *Mol. Phys.* **31**, 515 (1976).
- ²⁷A. R. Cooper, S. Jain, and J. M. Hutson, *J. Chem. Phys.* **98**, 2160 (1993).
- ²⁸L. Jansen, *Phys. Rev.* **125**, 1798 (1962).
- ²⁹A. R. Cooper, Ph.D. thesis, Durham University, 1992.
- ³⁰A. D. Buckingham, *Colloq. Internat. du CNRS* **77**, 57 (1959).
- ³¹R. D. Amos, *Chem. Phys. Lett.* **88**, 89 (1982).
- ³²P. Niyaz, unpublished work, 1996.
- ³³M. Lewerenz, *J. Chem. Phys.* **104**, 1028 (1996).
- ³⁴C. E. Dykstra, *J. Chem. Phys.* **108**, 6619 (1998).
- ³⁵S. Liu, Z. Bačić, J. W. Moskowitz, and K. E. Schmidt, *J. Chem. Phys.* **101**, 6359 (1994).
- ³⁶B. Schmidt and P. Jungwirth, *Chem. Phys. Lett.* **259**, 62 (1996).